Type of the Paper -Article

Title: Machine-Learning Reduced Order Model for Cost and Emission Assessment of a Pyrolysis

O. Olafasakin[1], Y. Chang[1], A. Passalacqua[1], Subramaniam S.[1], R. C. Brown[1,2], M Mba Wright[1,2,*]
[1]Department of Mechanical Engineering
[2]Bioeconomy Institute
Iowa State University
Ames, IA 50010
* Correspondence: markmw@iastate.edu; Tel.: 515-294-0913

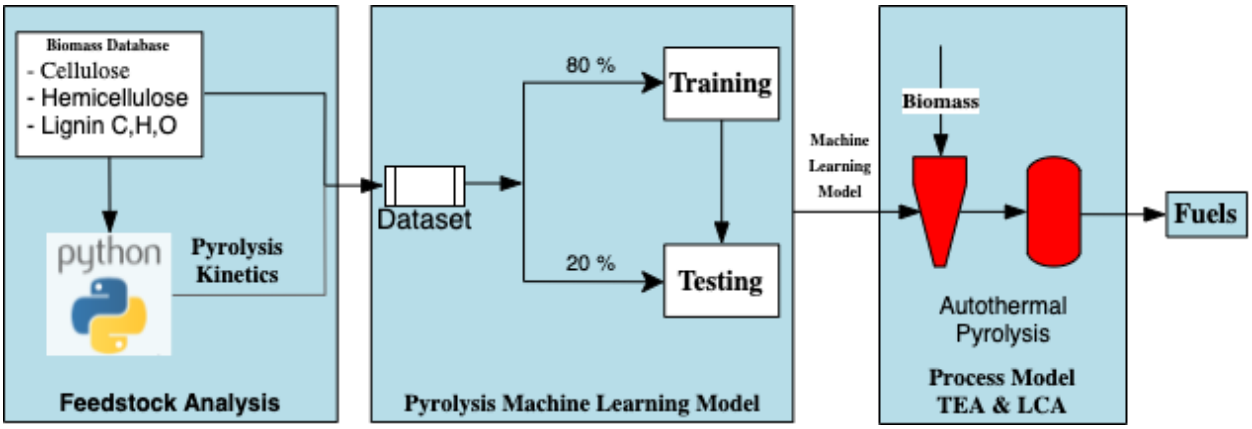

Abstract: Biomass pyrolysis is a promising approach for producing economic and environmentally-friendly fuels and bioproducts. Biomass pyrolysis experiments show that feedstock properties have a significant impact on product yields and composition. Scientists are developing detailed chemical reaction mechanisms to capture the relationships between biomass composition and pyrolysis yields. These mechanisms can be computationally intensive. In this study, we investigate the use of a machine learning reduced order model (ROM) for assessing the costs and emissions of a pyrolysis biorefinery.

We developed a Kriging-based ROM to predict pyrolysis yields of 314 feedstock samples based on the results of a detailed chemical kinetic pyrolysis mechanism. The ROM is integrated into a chemical process model for calculating mass and energy yields in a commercial-scale (2000 tonne/day) biorefinery. The ROM estimated biofuel yields of 65 to 130 gallons per ton of dry biomass. This results in biofuel minimum fuel-selling prices of $2.62 to $5.43 per gallon and emissions of -13.62 to 145 kg of CO_2 per MJ. The ROM achieved an average mean square error of 1.8e-20 and a mean absolute error of 0.53%. These results suggest that ROMs can facilitate rapid feedstock screening for biorefinery systems.

Keywords

Machine learning; Reduced order model; lifecycle assessment; Autothermal pyrolysis; biorefinery

1. Introduction

Recent increases in greenhouse gas emissions (GHG) have led to changes in natural climate patterns with significant economic, political, and societal impacts [1]. Transportation fuels are a significant source of these emissions, contributing 28% of global GHG emissions [2]. Several public policies have been developed, such as the Renewable Fuels Standard (RFS2) [3], to incentivize GHG reduction from the transportation sector. Biomass has been identified as one of the most promising energy sources to achieve this goal [4]. First-generation biofuels like corn ethanol have met the targets of the RFS2. However, advanced cellulosic biofuel production remains limited due to several techno-economic challenges [5]. In particular, thermochemical technologies such as pyrolysis remain under development to address the variability in lignocellulosic feedstock composition [6,7].

Feedstock composition can significantly impact biofuels' yield and quality [8], and low biofuel yields contribute to the high costs of advanced cellulosic biofuels. Scientists are investigating the impact of feedstock composition on pyrolysis product yields and biofuel cost[9,10]. Li et al. investigated the effects of 346 different feedstock samples on pyrolysis minimum fuel-selling price and greenhouse gas emissions using a linear regression model based on experimental data. They reported that the minimum fuel selling price (MFSP) varied between $2.3/gal and $4.8/gal, and GHG reductions compared to petroleum emissions (93 g/CO_2 e/MJ) ranged from 85% to 98%. They determined that ash content, followed by oxygen content, has the most significant impact on yields. Meyer et al. evaluated the process economics and GHG emissions for the fast pyrolysis of eleven biomass feedstocks, followed by pyrolysis oil upgrading via deoxygenation to produce transportation fuels. They used a CHEMCAD^{TM} process model and data from previous experimental studies to determine pyrolysis products. They found that capital-related costs

contributed the most to the MFSP (30% - 40%). They also recorded that the highest product yield is from pine feedstock, and the lowest is from switchgrass feedstock [9].

Most previous studies have employed statistical regression or interpolation from experimental data to predict pyrolysis products [9,10]. Few studies have applied machine learning techniques to pyrolysis and other bio-renewable energy conversion processes. Even fewer studies have employed modern machine learning techniques to the process models used in evaluating the TEA and LCA of biofuels. Hansen & Mirkouei published a comprehensive review of the past infrastructure and machine intelligence for biofuel production [11]. They compared cyber-physical systems, artificial intelligence, and machine learning techniques, and they reported that machine learning techniques appear to be more proven and better suited for applications in pyrolysis [11].

Hough et al. evaluated the ability of decision trees and artificial neural network machine learning models to predict pyrolysis reactions [12]. They employed maximum temperature, heating rate, and mass fractions of carbon and hydrogen in the lignin feedstock as the machine learning training data. They were able to reduce the computational expense of detailed kinetic models by four orders of magnitude. They employed mean squared error (MSE) and R-square as the prediction evaluation metrics. Aydinli et al. used artificial neural networks to predict the pyrolysis primary products char, tar, and gas based on the feedstock cellulose, hemicelluloses, and lignin, and ash, fix carbon volatiles, moisture, and pyrolysis reaction temperature as inputs. They used experimental data from the pyrolysis of Cotton-s, Tea-w, Olive-h, and Hazelnut-s at various temperatures to generate a training and testing dataset. The model was evaluated using the MSE method[13]. Tang et al. applied and compared multiple linear regressions and random forest

algorithms to forecast the bio-oil yield and hydrogen content of bio-oil using proximate and ultimate analysis of the biomass composition and pyrolysis conditions as input [14]. They investigated the properties that exert the most influence on the biofuel yield and hydrogen content of bio-oil. The two models' performance was evaluated using the MSE and coefficient of determination (R^2) between the predicted yields and the test dataset's actual yields.

Merdun & Sezgin employed two different types of artificial neural networks to model pyrolysis product yields. They trained a feed-forward network (FFN) and a cascade-forward network (CFN) to predict the pyrolysis process's biochar, bio-oil, and gas mixture content of the products. The input parameters used in the study include the moisture content, volatile organic content, proximate analysis, ultimate analysis, higher heating value, heating rate, and temperature. The models were evaluated using the coefficient of determination, root MSE, and the mean error [15]. Other studies have also employed machine learning techniques in modeling biomass technologies ranging from pyrolysis to gasification and other technologies [16–23]. Table 1 shows a summary of machine learning studies found in the literature for biomass thermochemical conversion. These studies have proven that machine learning models can accurately predict pyrolysis performance and other thermochemical energy conversion processes.

Table 1.Summary of literature studies employing machine learning for investigating biomass thermochemical conversion

Biomass Type(s)	**Biomass Technology**	**Machine Learning Technique**	**Evaluation Method**	**Reference**
Lignin Feedstock	Pyrolysis	Artificial neural networks Decision Tree	MSE	[12]
Cotton-s Tea-w Olive-h Hazelnut-s	Pyrolysis	Artificial neural networks	MSE	[13]
Multiple feedstocks	Pyrolysis	Multiple linear regression Random forest	R-squared RMSE	[14]

Multiple feedstocks	Pyrolysis	Artificial neural networks	R-squared RMSE Mean error	[15]
Cattle manure	Pyrolysis	Artificial neural network least square support vector machine	Average percent relative error Average absolute percent relative error RMSE R-squared	[19]
Multiple feedstocks	Pyrolysis	Artificial neural network Support vector machine	Mean absolute error RMSE R-squared	[17]
Multiple feedstocks	Gasification	Random forest Least square support vector machine	RMSE Normalized RMSE	[16]
Olive pit	Gasification	Linear regression K nearest neighbor regression support vector machine regression Decision tree regression	MSE MAE R-squared	[22]
NA	Pyrolysis	Artificial neural network	MSE R-squared	[24]
Multiple feedstocks	Pyrolysis	Random forest regression	RMSE R-Squared	[23]

Machine learning models accelerate the prediction of process yields and improve computational chemical process model unit ’operations’ accuracy given appropriate training data. Some studies have designed computational pyrolysis reactor units to calculate pyrolysis products’ yield in real-time within various process modeling tools. Trendewicz et al. developed a state-of-the-art biomass pyrolysis kinetic mechanism based on Ranzi’s kinetics combined with the 1-D Eulerian fluid dynamics and heat transfer description to calculate the products of pyrolysis [25]. Humbird et al. further developed the model by designing a biomass fast pyrolysis reactor model with detailed reaction kinetics and 1-D fluid dynamics implemented in an equation-oriented modeling environment (Aspen Custom Modeler) [26]. They reduced the execution time and stability of the

model designed by Trendewicz et al. [25]. Reducing the execution time can help with rapid screening and assessment studies. Thus, there is an advantage in combining machine learning with computational chemical process simulation. However, there is a literature gap in using machine learning models to predict process performance in terms of the economic and environmental assessment of biofuel systems.

This study makes four contributions to the literature: 1) we develop a Kriging reduced order model (ROM) of the Ranzi et al. 2017 biomass autothermal pyrolysis (ATP) kinetic model, 2) we incorporate the ROM into an Aspen Plus unit operator via the CAPE-OPEN interface (AmsterCHEM, 2020), 3) we predict the ATP yield of 314 feedstock samples, and 4) we assess the costs and lifecycle emissions of transportation fuel production from a commercial-scale ATP biorefinery. To our knowledge, there is no available literature on the use of a Kriging CAPE-OPEN machine learning ROM unit operator to estimate the costs and GHG emissions of a biomass ATP biorefinery.

2. Materials and Methods

This study employs machine learning techniques to develop a Kriging reduced-order model based on a chemical kinetic model dataset. The Kriging model uses a Python module, PyKriging [28], that implements the Kriging statistical regression model [29]. The PyKriging model was trained and validated with an input-output dataset generated from a modified version of Ranzi et al.'s 2017 kinetic pyrolytic decomposition mechanism [30] Ranzi et al.'s 2017 pyrolysis model has been validated through numerous studies as a reasonable predictor of pyrolysis yields under typical operating conditions of about 500 °C and atmospheric pressure. The final machine learning ROM is coupled to a fast pyrolysis unit operator block within an Aspen Plus^{TM} chemical process model

of a biomass to gasoline biorefinery to estimate biofuel production rates. Mass and energy balances from the process model are gathered to calculate system performance, estimate unit operation and capital costs, and calculate lifecycle economic costs and greenhouse gas emissions as a function of feedstock composition. Figure 1 shows the workflow of this study.

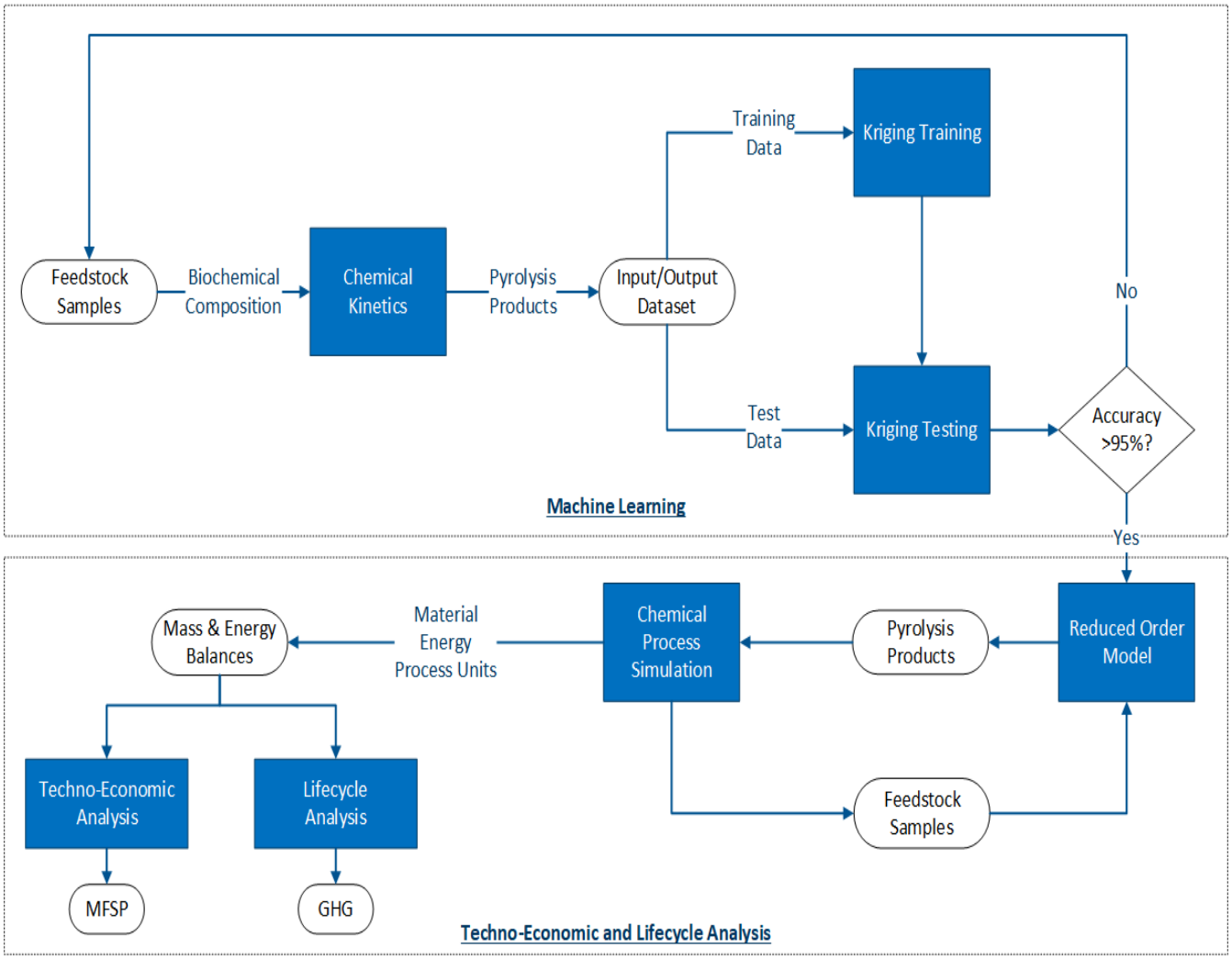

Figure 1. Machine learning (Kriging), lifecycle cost (TEA), and emissions (LCA) prediction framework for chemical process simulations with machine learning reduced-order models implemented using the CAPE-OPEN standard. Rounded rectangles represent data, filled squares represent software and sub-processes, and the diamond represents a decision step. Process outcomes include minimum fuel-selling price (MFSP) and greenhouse gas (GHG) emissions.

a. Data Generation and Collection

The dataset used to train the PyKriging models in this study was generated from a chemical kinetics model based on Ranzi's pyrolytic decomposition mechanism considered in Humbird et al. [26]. The chemical kinetics model's calculations are based on the dry ash-free feedstock composition considered in Humbird et al.'s work [26]. Ash content has a negative impact on pyrolysis oil yield and quality [10], but there are methods available to mitigate these impacts [31]. Comprehensive chemical kinetic models that address ash content's impacts on pyrolysis yields are limited by the significant variability caused by the presence of small (<5 wt.%) amounts of ash. This study's kinetic model assumes that the biomass consists of cellulose, hemicellulose, carbon-rich lignin, hydrogen-rich lignin, and oxygen-rich lignin. Biomass lignin in the dataset consists of equal quantities of carbon-, hydrogen-, and oxygen-rich lignin. This approach follows Ranzi et al.'s studies, and it is recommended when data is limited. Ranzi et al.'s kinetic model, as modified by Humbird et al.[26], contains 19 reactions and 33 compounds with five reactions for the decomposition of the biomass components into pyrolysis intermediate compounds. The intermediates further decompose into 21 pyrolysis products[26] . To account for char combustion, which provides the process heat for autothermal pyrolysis (ATP), the reaction shown in equation one was added to the chemical kinetics equations. The equation and the kinetic parameters: reaction rate, and activation energy were adapted from [35].

$$Char + O_2 \rightarrow CO_2 \qquad 1.2 * 10^{10}\ (-32300/RT) \qquad (1)$$

The model was implemented in Python and used to solve the computationally-intensive ordinary differential equations (ODE) to estimate the primary yields of autothermal pyrolysis. The input dataset supplied to the chemical kinetics model was generated using the python library Numpy's random function. The generated input dataset was subject to some conditional statements to

cover every possible percentage weight composition of cellulose, hemicellulose, and lignin contents of biomass to avoid bias. A total of 400 input data was generated and fed into the chemical kinetic model to calculate the corresponding ATP products. This resulted in a dataset of 400 input-output samples.

The input-output dataset was randomized and split into a training set and a test set with the ratio 8:2, which resulted in 320 input-output learning pairs and an 80 input-output test set. The model was trained with the training set and validated with the test set, which was not exposed to the model during training.

b. PyKriging Model Training, and ROM Development and Implementation

The machine learning (ML) model was developed using the PyKriging python module [28]. The Kriging method, also known as the Gaussian process regression method, is a metamodeling technique that employs the Gaussian process to develop mathematical piece-wise linear equations representing interpolation of the input data based on prior covariances [32]. The Kriging method has been applied to various spatial analysis applications and computer experiment applications [33–35]. However, it has not been used extensively for modeling pyrolysis reactions.

The PyKriging models were trained using the 314 input-output training pairs for the twenty-one primary products of ATP. The 21 PyKriging models were combined in a python function to develop the ROM. The individual PyKriging models were evaluated by comparing the predicted values with the actual values from the chemical kinetics using the coefficient of determination (R-

squared), mean absolute percentage error (MAPE), and root means squared error (RMSE). Equations 3 and 4 show the formula for computing the RMSE and MAPE.

$$RMSE = \sqrt{\frac{\sum_{i=1}^{n}(y_i - \bar{y}_i)^2}{n}} \quad (2)$$

$$MAPE = \left(\frac{\sum_{i=1}^{n}\frac{y_i - \bar{y}}{y_i}}{n}\right) * 100\% \quad (3)$$

Where n, y_i , and $\overline{y}_i$ are the number of observations, the actual value from the chemical kinetics model, and the predicted value from the PyKriging model, respectively.

The ROM was coupled with an Aspen Plus™ process model through a Computer-Aided Process Engineering open (CAPE-OPEN) interface [27]. CAPE-OPEN is an international standard for the interoperability of process modeling software. The CAPE-OPEN unit operator developed by AmsterCHEM allows for the integration of an Excel calculator block within an Aspen Plus™ flowsheet. Through the CAPE-OPEN interface, we can calculate the ATP product composition using the python machine learning model within a chemical process model. The CAPE-OPEN interface enables pyrolysis product calculations through an Excel workbook by sending the input stream's information to the workbook. The PyKriging model receives the biomass's input composition from the Excel workbook and returns the predicted output stream information to the Excel workbook. The CAPE-OPEN interface subsequently extracts the ATP's product stream information from the Excel workbook and sends the ATP's product stream information back to the process modeling tool. This process can be automated through the Aspen Plus automation interface to automatically run multiple simulations.

c. Process Modeling

The biorefinery process model was developed in Aspen Plus™. The process model simulates a biorefinery capable of processing 2000 metric tons per day (MT/d) biomass. The design and unit descriptions are described in detail in the paper by Li et al. [10]. In this study, we employ an ATP unit [36] instead of the conventional pyrolysis unit.

The system includes unit operations such as drying, grinding, autothermal pyrolysis, stabilization, and hydroprocessing. Figure 2 shows a simplified process flow diagram of the system. In summary, the biomass feedstock is first dried to less than 10 wt% moisture content. Then, ground to a screen size of less than 3 mm, and finally fed into an ATP reactor operating at 500 ^{o}C with a reactor residence time of 2 to 5 seconds. The ATP products are recovered as heavy end, light end, and non-condensable gas streams. The heavy end is first stabilized before hydroprocessing to produce gasoline and diesel range blend-stock fuels. Light ends and non-condensable gases are sent to the gas burner to generate process heat for biomass drying. Details about this process are available in the article by Li et al. [10].

The autothermal pyrolysis (ATP) unit was recently developed by Polin et al. [36]. It employs oxygen at an equivalence ratio of 0.10 to partially combust biomass compounds and directly provide process heat within the pyrolysis reactor. This approach reduces the reactor's energy input requirement and allows the pyrolysis unit to operate without external heat sources. As shown in Polin et al.'s study, ATP yields of desirable products are within 10% of conventional pyrolysis yields. ATP oxygen's requirement depends on the oxygen concentration of the flow gas and the input biomass composition. However, a fixed baseline equivalence ratio of 0.20 was employed in this study. This baseline equivalence ratio is enough for most cases to have sufficient oxygen for ATP operation, but some feedstock may need additional oxygen or heat input.

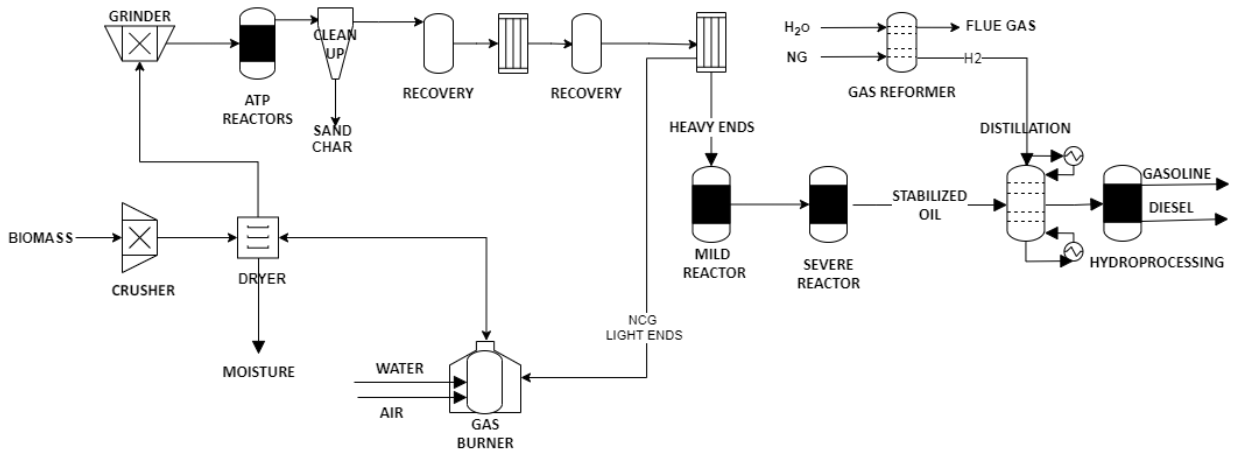

Figure 2. Biomass autothermal pyrolysis (ATP) for gasoline and diesel production

The ATP effluents are recovered as heavy ends and light ends through fractional distillation described in [37]. The heavy end is collected at 125^{o}C and consists of water-soluble sugars and water-insoluble phenolic oligomers. The light ends, which include water and acids, are collected at 15^{oC}. The light ends, and the non-condensable gases from ATP are sent to the gas burners to generate process heat for drying biomass. The heavy end is stabilized through a two-step stabilization process described in [37]. The heavy ends were sent to a mild reactor where the heavy ends are stabilized via mild hydrotreating over cobalt molybdenum catalyst at a pressure of 121 bar and a temperature of 140^{o}C. The output is further stabilized in a severe reactor at a pressure of 121 bar and a temperature of 370^{o}C to produce stabilized oil, wastewater, and off-gas streams. The stabilized oil is further processed into gasoline and diesel through fractional distillation.

d. Feedstocks for Economic and Life Cycle Analysis

The biomass dataset contains 320 feedstock samples, including herbaceous, woody, and oily feedstock types. The feedstock samples were characterized by their biochemical composition (cellulose, hemicellulose, and lignin compositions). The cellulose content of the sampled feedstock ranges between 0.03 and 100 wt.%. The hemicellulose content ranges between 0 and 83.3 wt.%. **Figure *3*** shows a Van Krevelen type diagram cross plotting the Lignin/Cellulose wt.%

ratio as a function of the Hemicellulose/Cellulose Wt.% ratio. Grass plants tend to have low Hemicellulose/Cellulose and Lignin/Cellulose ratios with a few exceptions. Husk shell pit and untreated wood have the widest spread in terms of both ratios. Organic residue has low Lignin/Cellulose ratios but a wide range of Hemicellulose/Cellulose ratios. All biomasses whose cellulose, hemicellulose, and lignin contents account for less than thirty percent of the total biochemical composition were filtered out of the feedstocks to avoid underestimating the potential yield. The filtered out biomass was removed because the PyKriging model predicts the ATP output based on the cellulose, hemicellulose, and lignin content. Twenty-six feedstocks were filtered thereby reducing the feedstock samples to 314.

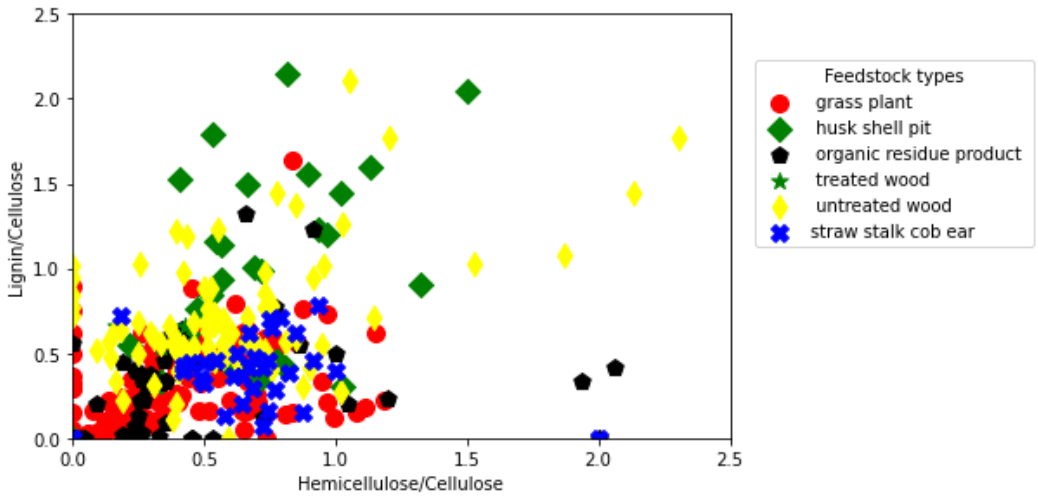

Figure 3. Van Krevelen type diagram showing the feedstock hemicellulose/cellulose and lignin/cellulose ratios of 340 biomass samples [38]

e. Economic Analysis

The techno-economic analysis (TEA) in this study employs guidelines developed by the U.S. Department of Energy for evaluating the economic potential of biofuel production pathways [39]. This study assessed the minimum fuel-selling price (MFSP) of all the feedstocks. The MFSP is the fuel price required to achieve a net present value (NPV) of zero at a 10% internal rate of return based on the discounted cash flow rate of return (DCFROR) method. The capital cost, a one-time expenditure used to purchase and install all process equipment, was calculated using Aspen Plus Economic Analyzer (APEA) estimates and other public data sources. Data from past TEA studies on pyrolysis platforms were employed to calculate expenses for custom-engineering units [40–43]. Scale-up ratios were applied to assess commercialized plants' purchasing costs, as recommended in Peters and Timmerhaus's [44]. For the financial assumptions, the study employed "n^{th}" plant assumptions, which assume that the necessary engineering breakthroughs and technical innovations required for reliable commercial operation have been achieved. All financial assumptions are tabulated in Table 2. To finance the project, a 40% percent equity is assumed, and the remaining 60% is taken as a loan to be paid back in ten years at an interest rate of 10%. The contingency accounting for all unexpected expenses due to unforeseen events is assumed to be 9.5% of the total purchase and installation cost. All costs and estimates were made on a 2011 rolling dollar basis.

Table 2. Techno-economic analysis financial assumptions

Parameters	Financial Assumptions
Equity	40%
Interest rate for financing	10%
Term for debt financing	10 years
Income tax rate	39%

Internal rate of return	10%
Plant life	
Construction period	3 years
Depreciation period	7 years MACRS schedule
Working capital	20% of Fixed capital cost
Project contingency	10% of Fixed capital cost
Plant salvage value	$0
Start-up time	0.5 years
Revenue and cost during start-up	50% of normal revenue 75% of normal variable cost 100% of fixed cost
Electricity price	6.16 cents/kWh

The operating cost reflects the expenditures from operating the plant annually. Operating cost assumptions were adapted from reports by the National Renewable Energy Laboratory (NREL) [39,43] and tabulated in Table 3. Some of the critical operating cost assumptions include a cost of 18 cents /m^3 for natural gas. The hydrotreating and hydrocracking catalysts cost $5.89/lb, and $18.25/lb, respectively. Operating cost assumptions for waste disposal include 30.86 cents/kg for sand and ash, and 11 cents/kg for wastewater disposal.

Table 3. Operating cost assumptions (Adapted from [39,43]*)*

Material/Resource	Price/Value
Raw materials	
Natural Gas	18 ¢/m^3
Pyrolysis catalyst	5.89$/lb
Hydrotreating catalyst	18.25 $/lb
Hydrocracking catalyst	18.25 $/lb
Hydrogen plant catalysts	13¢/m^3 H2
Boiler chemicals	1.65$/lb
Cooling Tower chemicals	1.18$/lb
GVL	0.85$/kg
Waste Disposal	
sand & ash	0.014 $/lb
WWT	0.11$/kg COD

By-product credits	
Off-gas	$0
char	$20/M.T
Utilities	
Cooling Tower makeup	1.95 ¢/10^6 gal
Boiling Feed Water makeup	1.95 ¢/10^6 gal
Hydrogen Plant Process Water	1.95 ¢/10^6 gal
Electricity	6.16 cents/kwh

The prices of different feedstock types are grouped according to representative feedstock costs. The costs for corn stover, switchgrass, and wood were taken from Meyer et al., 2020 [9]. The prices for other feedstock types are assumed as the average cost of corn stover, switchgrass, and wood. This price includes the cost of the feedstock production and logistics involved in their delivery [9]. The feedstocks' costs are shown in Table 4. Key factors impacting feedstock costs such as feedstock category, location, cultivation, and regulations [45–48] were beyond the scope of this analysis. This work assumed the process design to be fixed and not vary per feedstock type. This may result in sub-optimal yields for some feedstock samples. The by-product, biochar, is considered to be sold at $20/M.T. based on its energy content and use as a coal substitute.

Table 4. Biorefinery gate delivered feedstock costs based on feedstock type (adapted from[49]*)*

Feedstock	Type	Cost ($/MT)
Corn stover	Straw stalk cob ear	86.3
Switchgrass	grass/plants	87.7
Clean pine/Tulip poplar/ Hybrid poplar	woody	110
Others	Husk/Shell/pit, Organic residue, sludge, solid biofuel manure	94.6

f. Life Cycle Analysis

A lifecycle assessment (LCA) of GHG emissions was conducted for all 314 different biomass cases. LCA is an established methodology for assessing the environmental impact of a product from the extraction and preprocessing of the raw material through production and manufacturing to the point of consumption, disposal, or recycling. This study's LCA approach follows the methodology and assumptions described in Li et al. [10]. Argonne National Laboratory-developed Greenhouse Gases, Regulated Emission, and Energy Use in Transportation (GREET.net) were employed to evaluate the GHG emissions for the ATP-gasoline-diesel platform [50]. The modeling boundary for this work is from field to wheels and is shown in Figure 4.

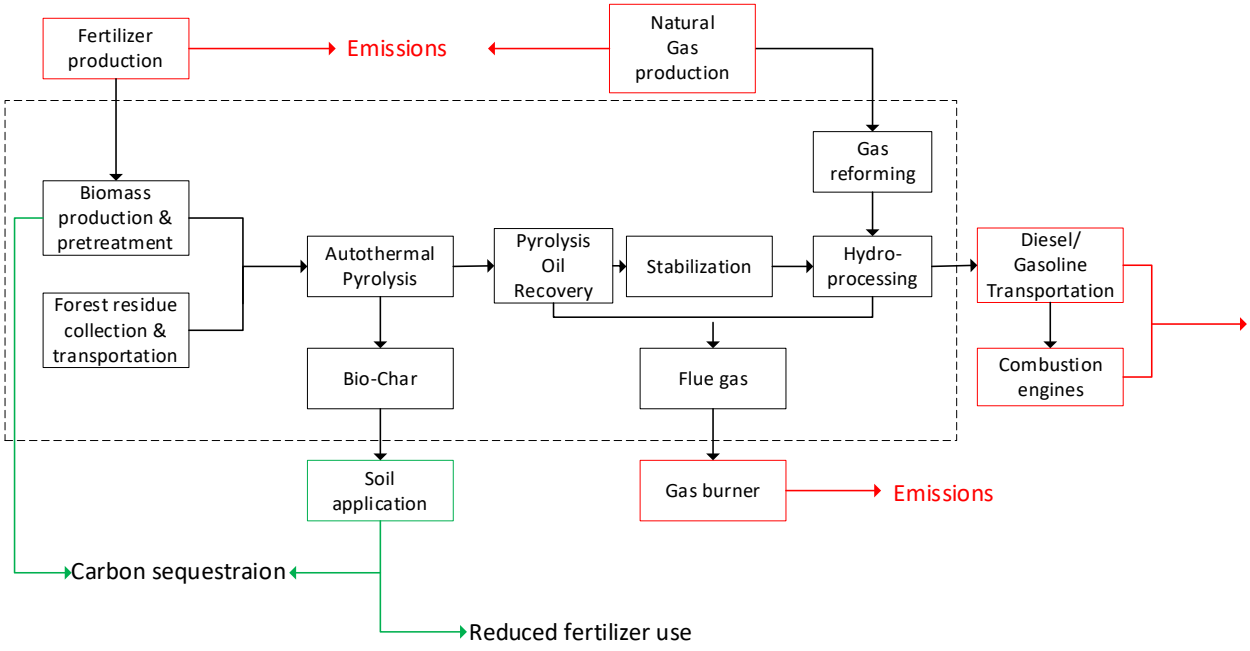

Figure 4. Lifecycle assessment system boundary for field-to-Wheels analysis of autothermal pyrolysis-based gasoline and diesel

The study assumes that the carbon uptake via photosynthesis during the growth of biomass compensates the emissions from processing and combusting produced fuel. Hence, biogenic carbon emissions were not considered. Material balance data were obtained from the process model, and other LCA analysis inventory data were obtained from GREET and SimaPro. Table 5 shows the LCA inventory and its sources. The four major hierarchy groups modeled in this analysis

include feedstock production, ATP, stabilization & upgrading, Hydrogen production, and fuel transportation. A higher heating value of 41.31 MJ/Kg is chosen as the heating value for the blended gasoline and diesel fuel based on the GREET software data are reported with a functional unit of 1 MJ of fuel produced to facilitate seamless comparisons with other LCA studies.

Table 5. Life Cycle Analysis emission factor inventory

		GHG Emission ($g CO_2$/kg input)	Source
Feedstock	Representative Feedstock		
Woody	Forest residue	45	GREET 2015
Straw	Corn stover	85	GREET 2015
Grass	Switch grass	140	GREET 2015
Organic residue	Bagasse	6	SimaPro 7
Husk	Palm Kernel	1400	SimaPro 7
Other emission sources			
Natural gas for heat production		2944	GREET 2015
Natural gas for hydrogen production		2790	GREET 2015
Fuel transportation		30	GREET 2015
Biochar sequestration		-1492	GREET 2015

Emissions associated with feedstock production include emissions from fertilizers and the petroleum fuel used during the cultivation and collection of biomass. The emissions in g $CO_{2,eq}$/kg involved in cultivating and processing biomass are gathered from GREET.net and SimaPro 7. Although GHG emissions associated with feedstock production vary due to differing cultivation and production requirements, this study represents each biomass category with a representative feedstock whose data is readily available due to limited emission data in the literature. The study assumed that the data for each category's representative feedstock represents all biomass that falls within that category. In this study, forest residue represents the wood category; corn stover represents straw; switchgrass represents grass; bagasse represents organic residue, and palm kernel represents the husk category. The study assumed that there was no fertilizer required for organic residue cultivation. Emissions associated with ATP, stabilization, and upgrading of biofuel are calculated in GREET. Emissions related to hydrogen production include emissions from natural gas production, transportation, and the steam reforming process. The emissions associated with fuel transportation include emissions from combusting fossil fuel in transporting the biofuel produced from the biorefinery to the terminals and ultimately to the retailing stations via heavy trucks. The emissions associated with these sources were taken from GREET. It is also worthy to note that the natural gas requirement for electricity usage during the processing of various feedstocks will differ by type. Still, this study assumed that the natural gas needed for electricity used for the process does not vary with the biomass yield. However, the natural gas requirements for the hydrogen plant vary with the biofuel yield.

3. Results and Discussion

a. Prediction Performance of the PyKriging ROM

The PyKriging models were trained to develop a ROM that predicts the primary products of ATP. After the training, the PyKriging model for each of the primary products of ATP was validated using the performance indicators MSE and MAPE. The MSE and MAPE were assessed based on how well the PyKriging model predicted the Python ODE-based kinetic model's output. The MAPE, MSE, and coefficient of determination values for the training set and the test set predictions for all the primary outputs of ATP are reported in Table 6. Similar results can be achieved with large experimental datasets. The PyKriging models showed approximately zero RMSE and zero MAPE for the training set and low values for the test set, as shown in Table 6. The largest MAPE recorded is 1.96%, and the largest RMSE recorded on the test set is 0.1633. These values were recorded for the model that predicts xylan. The largest MAPE recorded is much smaller than the MAPE of 5% reported in Li et al.[10]. This improvement is expected as Li et al.'s model estimated the LCA and TEA using a linear regression model. The coefficient of determination value shows that the models can predict the products of ATP with excellent accuracy. All PyKriging models showed a coefficient of determination score of approximately 0.99, which means the models predicted 99% of the variation in the simulated values from the chemical kinetic model. These accuracies match the accuracy reported in Hough et al., where a high R^2 of 99% and a low of 98% were recorded for the three algorithms considered in the study.

Table 6. Root-Mean Square Error (RMSE), Mean Absolute Percentage Error (MAPE) and, coefficient of determination (R-squared) of the pyrolysis product predictions from the chemical kinetics model.

Pyrolysis Products	**RMSE**	**MAPE**	**R-Squared**
Char	0.019	0.11	0.99
HAA	0.018	1.50	0.99
GLYOX	0.005	1.50	0.99
C3H6O	0.004	0.14	0.99
C3H4O2	0.002	0.26	0.99
HMFU	0.010	1.50	0.99
LVG	0.054	0.14	0.99
XYL	0.163	1.96	0.98

pCOUMARYL	0.003	0.13	0.99
PHENOL	0.001	0.11	0.99
FE2MACR	0.006	0.07	1.00
CH3CHO	0.003	0.56	0.99
ETOH	0.008	0.58	0.99
CH3OH	0.011	0.20	0.99
CO	0.050	0.57	0.99
CO2	0.046	0.39	0.99
CH4	0.013	0.34	0.99
CH2O	0.020	0.42	0.99
H2	~0.000	0.01	1.00
C2H4	0.009	0.22	0.99
H2O	0.007	0.16	0.99

Parity plots for the simulated values from the chemical kinetic model and the ROM machine learning's predicted values are shown in **Figure 5**. These plots show that the ROM and kinetic model predict similar values over a wide range of pyrolysis yields.

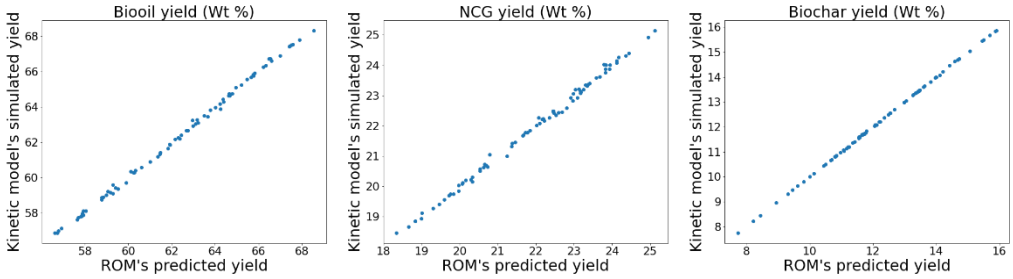

Figure 5. Parity plots comparing the Reduced Order Model (ROM) predicted and actual kinetic model outputs for a) biooil, b) biochar, and c) Non-Condensible Gas (NCG) for 314 feedstock samples.

The PyKriging ROM showed a satisfactory prediction performance of the bio-oil, Char and NCG. The PyKriging ROMs were used to estimate the ATP's yields of red oak. The yields were compared with the experimental values reported in Polin et al.[36], and the comparison is shown in Figure 6. The ROM showed a good agreement with the char values reported in Polin et al. but showed a slight difference in the values of biooil and NCG percentage weight values. This difference is due, in part, to the heavy and light end recovery simulation process, which can be optimized further depending on the bio-oil composition and intended product distribution.

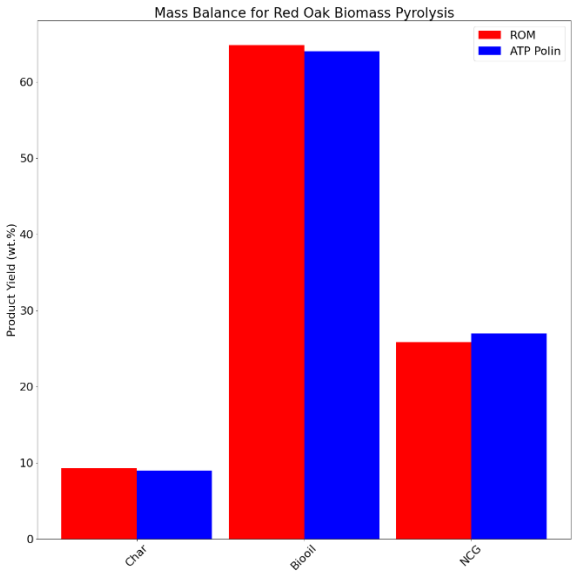

Figure 6. Comparison of ATP char, biooil, and Non-Condensible Gas (NCG) yields between the Reduced Order Model (ROM) (left) and autothermal pyrolysis (ATP) (right) experimental data reported by [36]

The PyKriging ROM model consists of binary python files. The binary files and code samples can be downloaded from GitHub via the link https://github.com/lumedee007/PyKriging-ROM-for-ATP. The binary files can be used to exercise the ROM as described in the methodology and used in estimating pyrolysis yields based on feedstock compositions. The model outputs can be employed in LCA and TEA models for the rapid screening of multiple feedstocks.

b. Process Modeling Results

The study employed an Aspen Plus^{TM} model to evaluate the biofuel yield of 314 feedstocks. The biorefinery process model results showed that biofuel yields could vary from 64.1 gallons of biofuel/tonne of biomass to 130 gallons of biofuel/tonne of biomass, depending on feedstocks. Figure 7 shows the effects of the biomass's biochemical composition on the biofuel yield of the biorefinery. The figure shows the impact of the cellulose content on the biofuel yield and biochar output. The biofuel yield increases as the biomass's cellulose content increase from zero to about

40% cellulose content. After 40%, an increase in cellulose content does not significantly affect the biofuel yield. There appears to be no definite relationship between the biomass's lignin to cellulose content ratio and the biofuel and biochar produced from the biomass. A limitation of this model is that feedstock with unusual compositions such as cellulose, hemicellulose, or lignin content below 5% can lead to yield estimates that are greater than 120 gallons/tonne or less than 40 gallons/tonne.

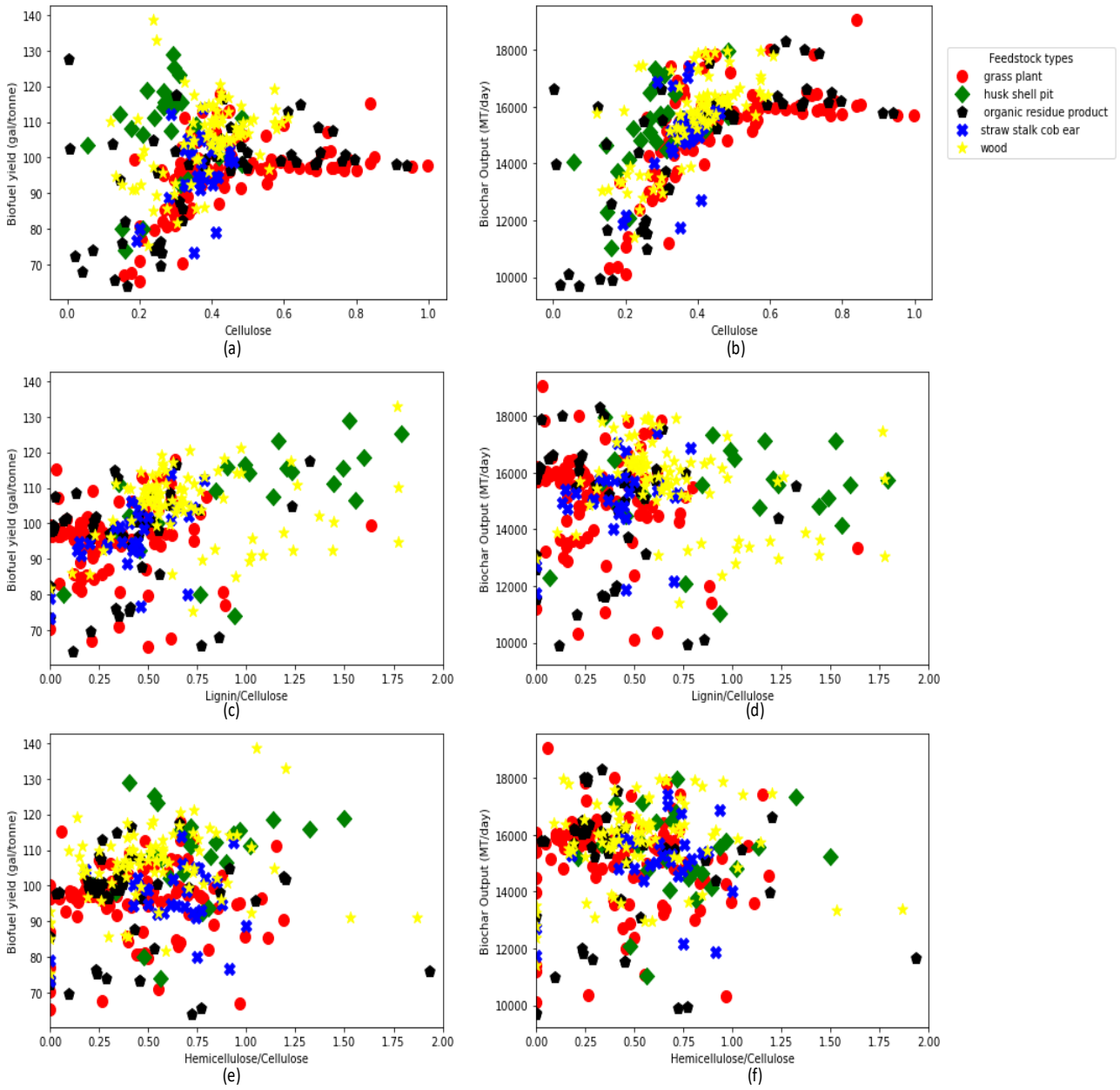

Figure 7. The impact of biomass' biochemical composition on the Biofuel yield and Biochar output (biomass are characterized into five types); (a,b) Impact of cellulose content on biofuel yield and biochar; (c,d) Impact of Lignin/Cellulose content on biofuel yield and biochar output; (e,f) Impact of Hemicellulose/cellulose content on biofuel yield and biochar output.

c. Economic Analysis Aesults

In this study, the MFSP was calculated for all 314 feedstocks. MFSP ranged from a minimum value of $2.62 to a maximum value of $5.43 per gallon of biofuel. Based on a 95% confidence

interval, the MFSP ranges from $3.55 to $3.66 per gallon. The average MFSP per feedstock category was estimated. Organic residue products have the largest mean MFSP at $3.78, and wood had the lowest at $3.30. Biofuel yield is the primary factor in the relationship between MFSP and feedstock type. Figure 8 shows the impact of the biochemical composition on the MFSP. Like the yield, cellulose appears to have a logarithmic relationship with the MFSP. Unlike the cellulose content, we could not establish a consistent trend or relationship between the MFSP and the Lignin/Cellulose.

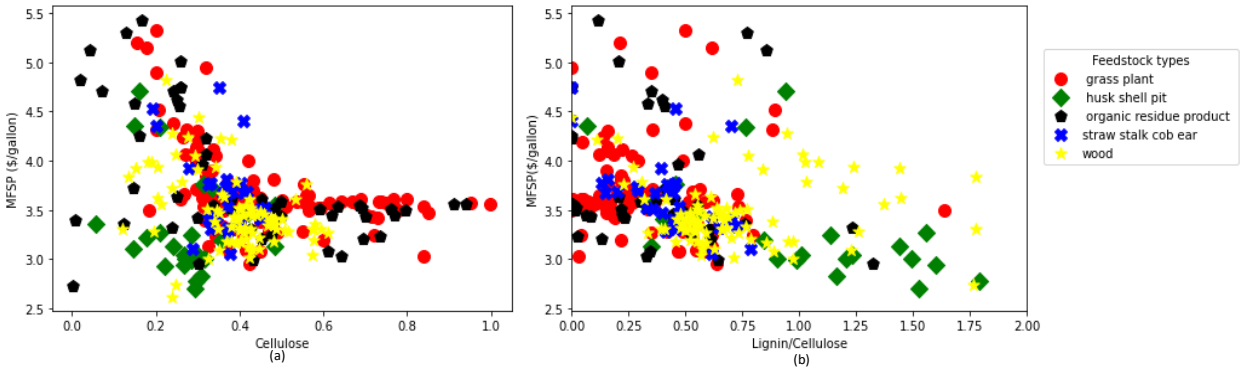

Figure 8. (a) Cellulose content impact on MFSP; (b) Lignin/Cellulose impact on MFSP

d. Life Cycle Analysis Results

This study evaluated the environmental impacts of producing biofuel from 314 feedstocks from the Phyllis database. Figure 9 shows the relationship between the cellulose content of the biomass and GHG emissions. The GHG emissions range from -13.62 to 145 kg of CO2/MJ. The graph shows that the GHG emissions of Husk/Shell/Pit are considerably higher than the other categories' GHG emissions. The average GHG emissions of the Husk/Shell/Pit category is 96.0 gm $CO_{2,eq}$/MJ, while the closest to it is grass/Plants at 1.0 gm $CO_{2,eq}$/MJ. The difference in GHG emissions is consistent with the results obtained by Li. et al. [10]. The difference between the GHG emissions of Husk/Shell/Pit and other biomass categories is due to the high contribution of the indirect land-

use change from food production. Furthermore, Husk/shell/pit achieves low biofuel yield, which further increases the carbon footprint.

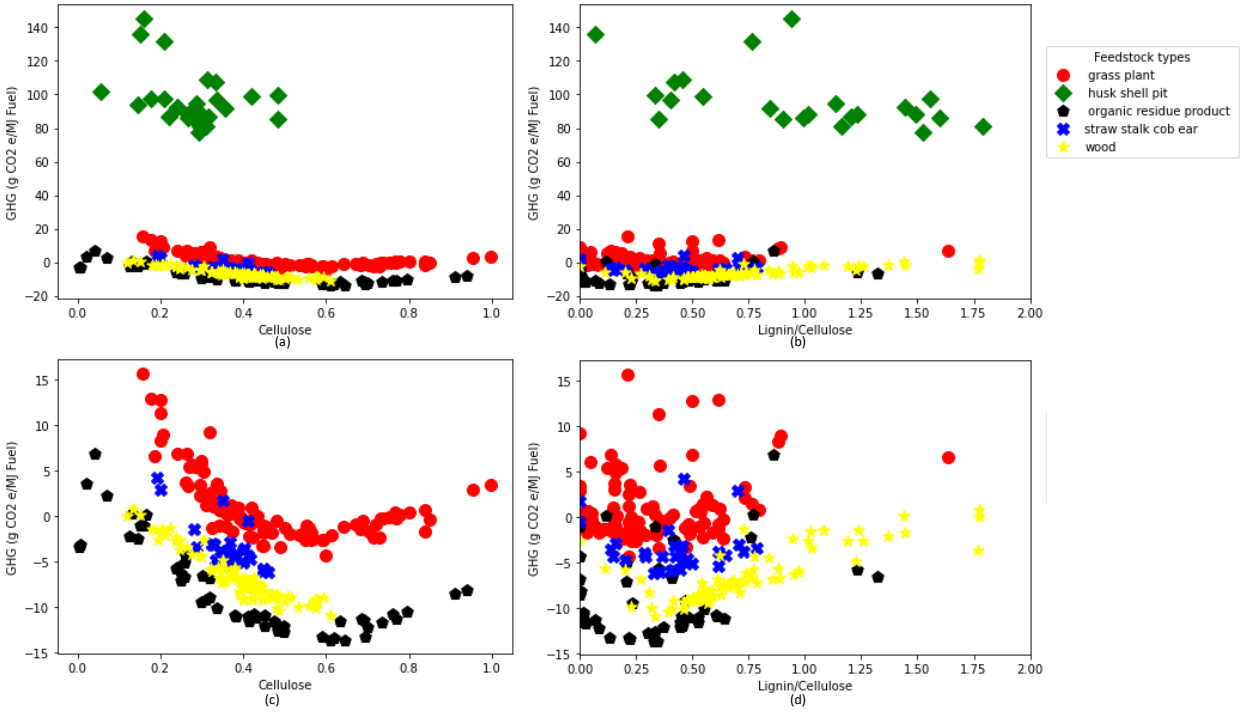

Figure 9. The impact of the biochemical composition of biomass on GHG emissions. (a,b) Impact of cellulose and lignin/cellulose on GHG emissions of all biomass categories; (c,d) Impact cellulose and lignin/cellulose on all categories excluding husk.

4. Conclusion

This study investigated the use of a reduced-order model (ROM) for predicting biofuel yields from a commercial-scale ATP biorefinery. The ROM is based on a Kriging machine learning model trained with an input-output dataset generated from an autothermal pyrolysis chemical reaction kinetic model. Predictions from the ROM are employed in a chemical process model to calculate the mass and energy balances of the ATP to gasoline and diesel process of 314 feedstock samples. Mass and energy balances are employed to calculate biofuel costs and emissions using techno-economic and lifecycle assessment.

Results indicate that the minimum fuel selling price can vary between $2.62 to $5.43 per gallon, and biofuel yields can vary from 64.1 to 138.8 gallons per ton of dry biomass. The GHG emissions vary between -13.62 to 145 kg of CO_2/MJ.

This study shows that a ROM can be successfully integrated into an ATP biorefinery process model in real-time to estimate gasoline and diesel yields. The ROM achieves high accuracy and facilitates rapid screening of biomass feedstocks based on their predicted costs and emissions. Future work is needed to incorporate other biorefinery operation factors that could influence its profitability and emissions.

Author Contributions: "Conceptualization, M.W. and O.O.; methodology, O.O. and M.M.; software, O.O.,M.M.; validation, M.M., and O.O.; formal analysis, M.M., and O.O.; investigation, M.M., and O.O.; resources, M.M., and O.O.; data curation, M.M., O.O, and Y.C.; writing—original draft preparation, O.O., and Y.C; writing—review and editing, M.M.,A.P.,R.C., and S.S.; visualization, O.O., AND Y.C.; supervision, M.M.; funding acquisition, M.M.,A.P.,R.C., and S.S. All authors have read and agreed to the published version of the manuscript.",

Funding: The authors would like to acknowledge the support of the U.S. Department of Energy through the grant DE-EE0008326.

REFERENCES

1. Pearce, D. The social cost of carbon and its policy implications. *Oxford Rev. Econ. Policy* **2003**, *19*, 362–384, doi:10.1093/oxrep/19.3.362.
2. US EPA, O. Fast Facts on Transportation Greenhouse Gas Emissions.
3. Renewable Fuel Standard (RFS): Overview and Issues - Randy Schnepf - Google Books Available online: https://books.google.com/books?hl=en&lr=&id=ZJcjNprDS3EC&oi=fnd&pg=PA1&dq=renewable+fuel+standard+2+rfs2&ots=hzTQ3plkRw&sig=llclGSIe4TJcnCVrufet_kDkpYc#v=onepage&q=renewable fuel standard 2 rfs2&f=false (accessed on Sep 15, 2020).
4. Hall, D.O.; House, J.I. Biomass: a modem and environmentally acceptable fuel. *Sol. Energy Mater. Sol. Cells* **1995**, *38*, 521–542, doi:10.1016/0927-0248(94)00242-8.
5. Tao, L.; Aden, A. The economics of current and future biofuels. In *Biofuels: Global Impact on Renewable Energy, Production Agriculture, and Technological Advancements*; Springer New York, 2011; pp. 37–69 ISBN 9781441971449.
6. Venderbosch, R.H.; Prins, W. Fast pyrolysis technology development. *Biofuels, Bioprod. Biorefining* 2010, *4*, 178–208.
7. Polin, J.P.; Carr, H.D.; Whitmer, L.E.; Smith, R.G.; Brown, R.C. Conventional and autothermal pyrolysis of corn stover: Overcoming the processing challenges of high-ash agricultural residues. *J. Anal. Appl. Pyrolysis* **2019**, *143*, 104679, doi:10.1016/j.jaap.2019.104679.
8. Williams, C.L.; Westover, T.L.; Emerson, R.M.; Tumuluru, J.S.; Li, C. Sources of Biomass Feedstock Variability and the Potential Impact on Biofuels Production. *Bioenergy Res.* **2016**, *9*, 1–14, doi:10.1007/s12155-015-9694-y.

9. Meyer, P.A.; Snowden-Swan, L.J.; Jones, S.B.; Rappé, K.G.; Hartley, D.S. The effect of feedstock composition on fast pyrolysis and upgrading to transportation fuels: Techno-economic analysis and greenhouse gas life cycle analysis. *Fuel* **2020**, *259*, 116218, doi:10.1016/j.fuel.2019.116218.

10. Li, W.; Dang, Q.; Brown, R.C.; Laird, D.; Wright, M.M. The impacts of biomass properties on pyrolysis yields, economic and environmental performance of the pyrolysis-bioenergy-biochar platform to carbon negative energy. *Bioresour. Technol.* **2017**, *241*, 959–968, doi:10.1016/j.biortech.2017.06.049.

11. Hansen, S.; Mirkouei, A. Past Infrastructures and Future Machine Intelligence (MI) for Biofuel Production: A Review and MI-Based Framework. In Proceedings of the Volume 4: 23rd Design for Manufacturing and the Life Cycle Conference; 12th International Conference on Micro- and Nanosystems; American Society of Mechanical Engineers, 2018; pp. 1–10.

12. Hough, B.R.; Beck, D.A.C.; Schwartz, D.T.; Pfaendtner, J. Application of machine learning to pyrolysis reaction networks: Reducing model solution time to enable process optimization. *Comput. Chem. Eng.* **2017**, *104*, 56–63, doi:10.1016/j.compchemeng.2017.04.012.

13. Aydinli, B.; Caglar, A.; Pekol, S.; Karaci, A. The prediction of potential energy and matter production from biomass pyrolysis with artificial neural network. *Energy Explor. Exploit.* **2017**, *35*, 698–712, doi:10.1177/0144598717716282.

14. Tang, Q.; Chen, Y.; Yang, H.; Liu, M.; Xiao, H.; Wu, Z.; Chen, H.; Naqvi, S.R. Prediction of Bio-oil Yield and Hydrogen Contents based on Machine Learning Method: Effect of Biomass Compositions and Pyrolysis Conditions. *Energy & Fuels* **2020**,

doi:10.1021/acs.energyfuels.0c01893.

15. Merdun, H.; Sezgin, I. V Modelling of pyrolysis product yields by artificial neural networks. *Int. J. Renew. Energy Res.* **2018**, *8*, 1178–1188.

16. Mutlu, A.Y.; Yucel, O. An artificial intelligence based approach to predicting syngas composition for downdraft biomass gasification. *Energy* **2018**, *165*, 895–901, doi:10.1016/j.energy.2018.09.131.

17. Chen, X.; Zhang, H.; Song, Y.; Xiao, R. Prediction of product distribution and bio-oil heating value of biomass fast pyrolysis. *Chem. Eng. Process. - Process Intensif.* **2018**, *130*, 36–42, doi:10.1016/j.cep.2018.05.018.

18. Xiong, Q.; Aramideh, S.; Passalacqua, A.; Kong, S.C. BIOTC: An open-source CFD code for simulating biomass fast pyrolysis. *Comput. Phys. Commun.* **2014**, *185*, 1739–1746, doi:10.1016/j.cpc.2014.02.012.

19. Cao, H.; Xin, Y.; Yuan, Q. Prediction of biochar yield from cattle manure pyrolysis via least squares support vector machine intelligent approach. *Bioresour. Technol.* **2016**, *202*, 158–164, doi:10.1016/j.biortech.2015.12.024.

20. Ozbas, E.E.; Aksu, D.; Ongen, A.; Aydin, M.A.; Ozcan, H.K. Hydrogen production via biomass gasification, and modeling by supervised machine learning algorithms. *Int. J. Hydrogen Energy* **2019**, doi:10.1016/j.ijhydene.2019.02.108.

21. Zhang, J.; Liu, J.; Evrendilek, F.; Zhang, X.; Buyukada, M. TG-FTIR and Py-GC/MS analyses of pyrolysis behaviors and products of cattle manure in CO2 and N2 atmospheres: Kinetic, thermodynamic, and machine-learning models. *Energy Convers. Manag.* **2019**, *195*, 346–359, doi:10.1016/j.enconman.2019.05.019.

22. Ozbas, E.E.; Aksu, D.; Ongen, A.; Aydin, M.A.; Ozcan, H.K. Hydrogen production via

biomass gasification, and modeling by supervised machine learning algorithms. *Int. J. Hydrogen Energy* **2019**, *44*, 17260–17268, doi:10.1016/j.ijhydene.2019.02.108.

23. Zhu, X.; Li, Y.; Wang, X. Machine learning prediction of biochar yield and carbon contents in biochar based on biomass characteristics and pyrolysis conditions. *Bioresour. Technol.* **2019**, *288*, 121527, doi:10.1016/j.biortech.2019.121527.
24. Zhong, H.; Xiong, Q.; Yin, L.; Zhang, J.; Zhu, Y.; Liang, S.; Niu, B.; Zhang, X. CFD-based reduced-order modeling of fluidized-bed biomass fast pyrolysis using artificial neural network. *Renew. Energy* **2020**, *152*, 613–626, doi:10.1016/J.RENENE.2020.01.057.
25. Trendewicz, A.; Braun, R.; Dutta, A.; Ziegler, J. One dimensional steady-state circulating fluidized-bed reactor model for biomass fast pyrolysis. *Fuel* **2014**, *133*, 253–262, doi:10.1016/j.fuel.2014.05.009.
26. Humbird, D.; Trendewicz, A.; Braun, R.; Dutta, A. One-Dimensional Biomass Fast Pyrolysis Model with Reaction Kinetics Integrated in an Aspen Plus Biorefinery Process Model. *ACS Sustain. Chem. Eng.* **2017**, *5*, 2463–2470, doi:10.1021/acssuschemeng.6b02809.
27. AmsterCHEM - Excel Unit Operation Available online: https://www.amsterchem.com/excelunitop.html (accessed on Sep 16, 2020).
28. GitHub - capaulson/pyKriging: Welcome to the User Friendly Python Kriging Toolbox! Available online: https://github.com/capaulson/pyKriging (accessed on Jul 22, 2020).
29. Jones D.R. A Taxonomy of Global Optimization Methods Based on Response Surfaces. *J. Glob. Optim.* **2001**, *21*, 39, doi:10.1023/A:1012771025575.
30. Ranzi, E.; Debiagi, P.E.A.; Frassoldati, A. Mathematical Modeling of Fast Biomass

Pyrolysis and Bio-Oil Formation. Note II: Secondary Gas-Phase Reactions and Bio-Oil Formation. *ACS Sustain. Chem. Eng.* **2017**, *5*, 2882–2896, doi:10.1021/acssuschemeng.6b03098.

31. Rollag, S.A.; Lindstrom, J.K.; Brown, R.C. Pretreatments for the continuous production of pyrolytic sugar from lignocellulosic biomass. *Chem. Eng. J.* **2020**, *385*, 123889, doi:10.1016/j.cej.2019.123889.
32. Jones, D.R. A Taxonomy of Global Optimization Methods Based on Response Surfaces. *J. Glob. Optim.* **2001**, *21*, 345–383, doi:10.1023/A:1012771025575.
33. Hesamian, G.; Akbari, M.G. A kriging method for fuzzy spatial data. *Int. J. Syst. Sci.* **2020**, 1–14, doi:10.1080/00207721.2020.1781288.
34. Qiu, S. Design of a low noise turbofan duct via an acoustic gradient-enhanced Kriging method. *Proc. Inst. Mech. Eng. Part C J. Mech. Eng. Sci.* **2020**, *0*, 095440622093364, doi:10.1177/0954406220933640.
35. Cattle, J.A.; McBratney, A.B.; Minasny, B. Kriging Method Evaluation for Assessing the Spatial Distribution of Urban Soil Lead Contamination. *J. Environ. Qual.* **2002**, *31*, 1576–1588, doi:10.2134/jeq2002.1576.
36. Polin, J.P.; Peterson, C.A.; Whitmer, L.E.; Smith, R.G.; Brown, R.C. Process intensification of biomass fast pyrolysis through autothermal operation of a fluidized bed reactor. *Appl. Energy* **2019**, *249*, 276–285, doi:10.1016/j.apenergy.2019.04.154.
37. Jones, S.; Valkenburg, C.; Walton, C. Production of gasoline and diesel from biomass via fast pyrolysis, hydrotreating and hydrocracking: a design case. *Energy* **2009**, 76, doi:PNNL-22684.pdf.
38. Phyllis2 - ECN Phyllis classification Available online:

https://phyllis.nl/Browse/Standard/ECN-Phyllis (accessed on Sep 16, 2020).

39. Humbird, D.; Davis, R.; Tao, L.; Kinchin, C.; Hsu, D.; Aden, A.; Schoen, P.; Lukas, J.; Olthof, B.; Worley, M.; et al. Process Design and Economics for Biochemical Conversion of Lignocellulosic Biomass to Ethanol: Dilute-Acid Pretreatment and Enzymatic Hydrolysis of Corn Stover. *Natl. Renew. Energy Lab.* **2011**, 1–147.

40. Zhang, Y.; Brown, T.R.; Hu, G.; Brown, R.C. Techno-economic analysis of monosaccharide production via fast pyrolysis of lignocellulose. *Bioresour. Technol.* **2013**, *127*, 358–365, doi:10.1016/j.biortech.2012.09.070.

41. Wright, M. Techno-economic, location, and carbon emission analysis of thermochemical biomass to transportation fuels. **2010**.

42. Owen, R.G.; Morgan, G.J. Process Design and Economics for the Conversion of Lignocellulosic Biomass to Hydrocarbon Fuels. *Clin. Lab. Haematol.* **1998**, *20*, 199–206, doi:10.1046/j.1365-2257.1998.00174.x.

43. Dutta, A.; Sahir, A.; Tan, E.; Humbird, D.; Snowden-swan, L.J.; Meyer, P.; Ross, J.; Sexton, D.; Yap, R.; Lukas, J. Process Design and Economics for the Conversion of Lignocellulosic Biomass to Hydrocarbon Fuels. NREL/TP-5100-62455 and PNNL-23823. *Nrel* **2015**.

44. Max S. Peters, Klaus D. Timmerhaus, R.E.W. *Plant Design and Economics for Chemical Engineers*; 5th ed.; McGraw-Hill Professional: New York, NY; ISBN 9780072392661.

45. Carpenter, D.; Westover, T.L.; Czernik, S.; Jablonski, W. Biomass feedstocks for renewable fuel production: A review of the impacts of feedstock and pretreatment on the yield and product distribution of fast pyrolysis bio-oils and vapors. *Green Chem.* 2014, *16*, 384–406.

46. Kevin Kenney; Kara G. Cafferty; Jacob J. Jacobson; Ian J Bonner; Garold L. Gresham; William A. Smith; David N. Thompson; Vicki S. Thompson; Jaya Shankar Tumuluru; Neal Yancey *Feedstock Supply System Design and Economics for Conversion of Lignocellulosic Biomass to Hydrocarbon Fuels: Conversion Pathway: Biological Conversion of Sugars to Hydrocarbons The 2017 Design Case*; 2013;

47. Jacobson, J.J., Roni, M.S., Cafferty, K.G., Kenney, K., Searcy, E., and Hansen, J. Feedstock Supply System Design and Analysis "The Feedstock Logistics Design Case for Multiple Conversion Pathways." *Idaho Natl. Lab. 194* **2014**.

48. Li, W.; Dang, Q.; Smith, R.; Brown, R.C.; Wright, M.M. Techno-economic analysis of the stabilization of bio-oil fractions for insertion into petroleum refineries. *ACS Sustain. Chem. Eng.* **2017**, *5*, 1528–1537, doi:10.1021/acssuschemeng.6b02222.

49. Meyer, P.A.; Snowden-Swan, L.J.; Jones, S.B.; Rappé, K.G.; Hartley, D.S. The effect of feedstock composition on fast pyrolysis and upgrading to transportation fuels: Techno-economic analysis and greenhouse gas life cycle analysis. *Fuel* **2020**, *259*, 116218, doi:10.1016/j.fuel.2019.116218.

50. Argonne GREET Model Available online: https://greet.es.anl.gov/ (accessed on Sep 10, 2020).